the FEBS Journal

Intermonomer cross-linking of F-actin alters the dynamics of its interaction with H-meromyosin in the weak-binding state

György Hegyi[1] and József Belágyi[2]

1 Department of Biochemistry, Eötvös University, Budapest, Hungary
2 Institute of Bioanalysis, University of Pécs, Hungary

Keywords
actin cross-linking; actomyosin interactions; EPR spectroscopy; heavy meromyosin

Correspondence
G. Hegyi, Department of Biochemistry, Eötvös University, Pázmány Péter sétány 1./C H-1117 Budapest, Hungary
E-mail: hegyi@cerberus.elte.hu

(Received 3 January 2006, revised 20 February 2006, accepted 22 February 2006)

doi:10.1111/j.1742-4658.2006.05197.x

Previous cross-linking studies [Kim E, Bobkova E, Hegyi G, Muhlrad A & Reisler E (2002) *Biochemistry* **41**, 86–93] have shown that site-specific cross-linking among F-actin monomers inhibits the motion and force generation of actomyosin. However, it does not change the steady-state ATPase parameters of actomyosin. These apparently contradictory findings have been attributed to the uncoupling of force generation from other processes of actomyosin interaction as a consequence of reduced flexibility at the interface between actin subdomains-1 and -2. In this study, we use EPR spectroscopy to investigate the effects of cross-linking constituent monomers upon the molecular dynamics of the F-actin complex. We show that cross-linking reduces the rotational mobility of an attached probe. It is consistent with the filaments becoming more rigid. Addition of heavy meromyosin (HMM) to the cross-linked filaments further restricts the rotational mobility of the probe. The effect of HMM on the actin filaments is highly cooperative: even a 1 : 10 molar ratio of HMM to actin strongly restricts the dynamics of the filaments. More interesting results are obtained when nucleotides are also added. In the presence of HMM and ADP, similar strongly reduced mobility of the probe was found than in a rigor state. In the presence of adenosine 5′[βγ-imido] triphosphate (AMPPNP), a nonhydrolyzable analogue of ATP, weak binding of HMM to either cross-linked or native F-actin increases probe mobility. By contrast, weak binding by the HMM/ADP/AlF_4 complex has different effects upon the two systems. This protein–nucleotide complex increases probe mobility in native actin filaments, as does HMM + AMPPNP. However, its addition to cross-linked filaments leaves probe mobility as constrained as in the rigor state. These findings suggest that the dynamic change upon weak binding by HMM/ADP/AlF_4 which is inhibited by cross-linking is essential to the proper mechanical behaviour of the filaments during movement.

The molecular motions of actomyosin, most notably those underlying muscle contraction, result from dynamic interactions between actin and myosin as driven by ATP hydrolysis. Within the force-producing cycle, the myosin head undergoes profound conformational changes. A detailed picture of the movements

Abbreviations
ABP, N-(4-azidobenzoyl) putrescine; AMPPNP, adenosine 5′[βγ-imido] triphosphate; ANP, N-(4azido-2-nitrophenyl) putrescine; CW EPR, conventional EPR; HMM, heavy meromyosin; maleimido-TEMPO, 4-maleimido-2,2,6,6-tetramethyl-1piperidinyloxy free radical; p-PDM, *N,N′-p*-phenylenedimaleimide; S1, myosin subfragment-1; ST EPR, saturation transfer EPR.

within the myosin head has been inferred from X-ray crystallographic data of myosin subfragment-1 (S1) crystallized in the presence of different ATP and ADP/P_i analogues, as well as from kinetic studies using site-specific reporter signal probes [1,2]. Other studies have shown structural and dynamic changes of actin filaments due to their interaction with myosin. Less well understood, however, is the nature of conformational changes that occur within the filament during force generation. On the basis of polarized–fluorescence measurement of ghost fibres labelled with ε-ATP, it was shown that both the elastic modulus of the filaments and the orientation of actin monomers change upon the addition of heavy meromyosin (HMM) [3]. In another study, glycerinated actin fibres labelled with fluorescent phalloidin were analysed by fluorescence–polarization spectroscopy. The development of isometric tension was accompanied by a small rotation of the constituent monomers within each actin filament [4].

Recent studies using polarization–fluorescence spectroscopy indicate that dye molecules attached to actin change their orientation and mobility during the course of actomyosin ATPase cycles. The weak versus strong binding of the myosin S1 domain to labelled actin filaments causes opposing changes in polarization parameters. Apparently, subdomain movement occurs during the transition between weak- and strong-binding states [5].

EPR studies of probes attached to actin filaments have shown internal rotation occurring on a microsecond timescale. The binding of myosin heads exerts a co-operative effect that further restricts rotational motion within the actin filaments [6–8]. Moreover, experiments using caged ATP show no evidence for a difference between weak- and strong-binding states [8]. Measurements made by anisotropy of fluorescence using a narrow-aperture confocal microscope yield contrary results: changes in actin orientation during the power stroke were found [9], furthermore fluorescence–polarization measurement of sliding filaments in an *in vitro* motility assay led to the conclusion that the sliding F-actin performs an axial rotation with one revolution per 1 μm sliding distance [10].

It would be particularly interesting to find that constraints upon the flexibility of actin filaments affect their functional properties. In this respect, cross-linking studies are relevant, as they provide detailed information on the relationship between the structure and dynamics of actin and its motility. Three site-specific cross-links are localized in actin filaments. Cross-links connect Gln41 to Lys119 [11] and Gln41 to Cys374 [12] among actin molecules within the same strand, and another cross-link between Cys374 to Lys191 [13] connects opposing strands in the actin filaments. All three cross-links similarly inhibit filament sliding speed and force generation in *in vitro* motility assays. By the same token, none changes the strong binding of myosin S1 to actin, nor do they alter the V_{max} and K_M parameters of actomyosin ATPase activity or the rates of ADP release from acto-S1 [14,15]. One interpretation is that constrained dynamic flexibility within filaments causes an uncoupling between force generation and other molecular processes of actomyosin interaction. We addressed this issue using EPR spectroscopy to follow the dynamics of cross-linked actin filaments and to examine the effect of HMM binding. The spin-labelled probe was 4-maleimido-2,2,6,6-tetramethyl-1piperidinyloxy free radical (maleimido-TEMPO) covalently attached to Cys374. The primary aim of the study was to find differences in the dynamics of the constituent actin molecules of cross-linked versus native filaments. We hope that the resulting data will give clues to the mechanism by which cross-linking decreases movement in the *in vitro* motility assay.

Results and Discussion

Rotational motion of spin labels in cross-linked actin filaments

It is known from earlier experiments that Cys374 incorporates > 90% of the labels under the conditions used in this study, proving that the labelling procedure was highly selective [6,7,16]. Both conventional (CW EPR) and saturation transfer EPR (ST EPR) measurements showed that the labels were rigidly attached to actin monomers, and indicated the motion of a larger domain in the monomer. According to our experiments, in F-form uncross-linked actin the hyperfine splitting constant $2A'_{zz}$, which depends upon the slow rotational motion of the attached label, was 6.835 ± 0.026 mT ($n = 8$), whereas the diagnostic ST EPR parameter L″/L was estimated to be ∼0.7 ± 0.1 ($n = 4$), which corresponds to a rotational correlation time of ∼50–60 μs. Very likely, the labels reflected the torsional motion of several associated subunits.

The cross-links between the monomers by bifunctional reagents in F-actin imposed constrains on the structure, which influenced the internal motion of the protein (Fig. 1). Both inter- and intrastrand cross-links significantly affected the rotational motion of labels as measured by ST EPR. The intrastrand cross-links Gln41–Cys374 and Gln41–Lys113 seemed to produce a significantly larger decrease in the mobility of the

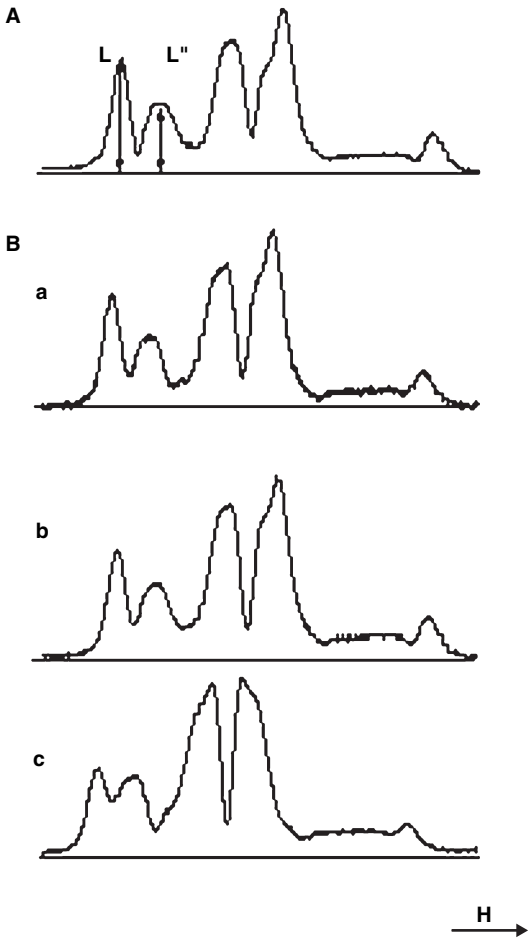

Fig. 1. ST EPR spectra of F-actin in native (A) and cross-linked (B) filaments. To generate such filaments, covalent attachment of the spin label to residue Cys374 of actin and cross-linking within/between protein subunits were accomplished as described in Experimental procedures. Each sample was contained in a flat cell oriented parallel to the magnetic field vector H. This geometry minimized distortion of the signal due to incomplete alignment of F-actin filaments. (B) shows the spectra of filaments of F-actin with three sorts of cross-links: (a) interstrand cross-links from Cys374 to Lys191; (b) intrastrand cross-links from Gln41 to Lys113; (c) intrastrand cross-links from Gln41 to Cys374.

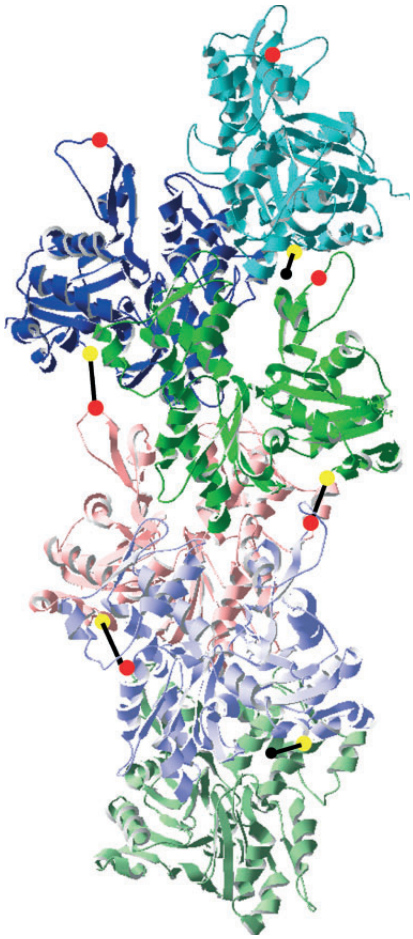

Fig. 2. Copolymer of Cys374/maleimido-TEMPO labelled and Gln41–Cys374 cross-linked actin. A segment of actin filament built up from six monomers is shown with different colours using PDB 1MVW data. Yellow and red spheres are assigned Cys374 and Gln41, respectively. Black lines show cross-links between Gln41 and Cys374 residues located on neighbouring monomers in the same actin strand. Black spheres symbolize the EPR probe attached to the Cys374 residue. Cross-linked and EPR probe labelled sites distribute randomly within the filaments, the estimated ratio of cross-linked and uncross-linked interfaces is about 1.5 : 1.

labels than the interstrand cross-links Lys191–Cys374, which evoked only a moderate change. Information regarding the localization of the three cross-links within the actin filaments in either the same or the opposing strand has been published previously [12,13,15]. Here, for clarity, the position of the EPR reporter group and one type of cross-link in the used copolymer is depicted in Fig. 2.

Decreases in the rotational motion of the labels suggest an overall restriction of the flexibility in cross-linked filaments. In the copolymers, subdomain 1, where the spin probe is attached, is not directly involved in the intermonomer cross-link, because one of the cross-linking sites is occupied by the spin probe, therefore, the rigidity of the cross-links between neighbouring monomers may affect the changes in the motion of the probes. The estimated ratio of cross-linked to uncross-linked interfaces is $\sim 1.5 : 1$, based on the composition of the copolymers (see Experimental procedures) and SDS/PAGE analysis of the efficiency of the cross-linking reaction. In addition to the change in the dynamics of the filaments, some torsion

in the geometry at the interfaces of the cross-linked monomers cannot be excluded. However, earlier studies have shown no significant distortion in F-actin structure in the case of Gln41–Cys374 [14,15] and Lys191–Cys374 cross-links [13], but on the basis of the positive cooperation of the cross-link formation between Gln41 and Lys113 some structural change was considered [15]. For this reason, we did not perform a detailed investigation of the interaction between myosin fragments and actin filaments cross-linked between Gln41 and Lys113.

Orientation dependence of EPR spectra of cross-linked actin

Actin filaments prepared using various techniques self-assemble into an ordered structure. The resulting geometry of spin-labelled actin is expected to influence the EPR spectrum. Oriented actin filaments can be prepared by flow through a capillary tube, by diffusion of actin monomers into muscle fibres or by careful smearing of an actin pellet onto the surface of a Zeiss flat cell [17,18]. Electron microscopy observations confirm that the last method produces well-oriented actin filaments. Two populations of probe molecules are detected in such an oriented system, one is highly ordered and the other relatively disordered [8,18,19]. Analysis of EPR spectra allowed derivation of the orientation distribution of spin labels, where the *z*-axis of the molecular reference system fits a Gaussian distribution [8]. Our analysis on experimental spectra showed that the angle between the principal *z*-axis of the spin label and the filament long axis was 34 ($\pm$3)° with a full width of 23° at half maximum of the distribution (Fig. 3). The second population of spin labels that was relatively disordered had a mean angle of 63 ($\pm$5)° with a full width at half maximum of 43°. For the sake of comparison, actin pellets were prepared from different samples, and EPR spectra were recorded on partially oriented gels in the Zeiss flat cells (Fig. 4). By rotating the flat cell, the filament long axis (k) is oriented either parallel (H par. k) or perpendicular (H per. k) to the laboratory magnetic field, and the ratio of the hyperfine splitting constants is compared (Table 1). The ratio of the hyperfine splitting constants can be used as a simple order parameter for comparison of different samples, because this ratio reflects the change in the angular distribution of the attached labels. In the case of a random distribution of probe molecules this ratio is equal to one. The intrastrand cross-links produce a significantly larger change in the orientation of the attached probe molecules than do interstrand cross-links. In all three cases, the locations of the probe molecules are relatively far

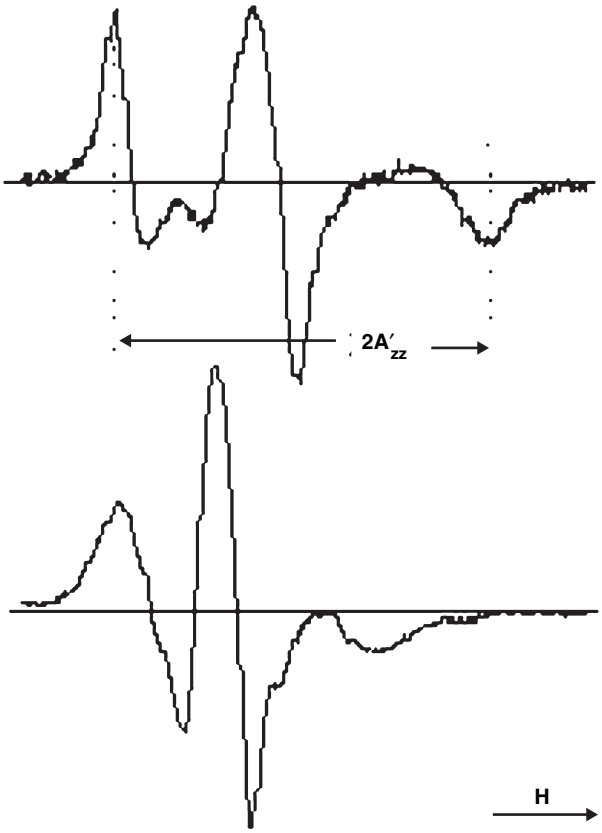

Fig. 3. Conventional EPR spectra of native F-actin filaments. A gel of this protein was applied to the surface of a flat spectroscopy cell. EPR spectra were recorded with this surface of the cell oriented parallel (upper) or perpendicular (lower) to H. The signal from the latter sample was corrected; the population arising from inexact alignment among F-actin filaments was subtracted. The resulting spectrum reveals the distribution of orientations among the attached spin labels. The quantity $2A'_{zz}$, the hyperfine splitting constant, is indicated on the magnetic field-axis.

from the spatial localization of the cross-links, but the imposed constraints affect the orientation of the probe molecules. The disorder can arise either from disorder of a local region of the protein or from improper orientation of the filaments. X-Ray diffraction experiments led to the conclusion that the disordered component might arise from disorder within an ordered filament [19].

Effects of cross-linking on the interaction of actin and myosin fragments

It is known that the addition of small amounts of HMM to actin filaments immobilizes the probe within a rigor complex. The hyperfine splitting constant peaks at a molar ration of $\sim$0.2 HMM/actin, then decreases

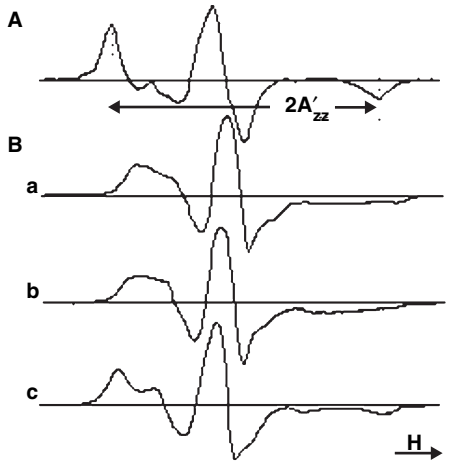

Fig. 4. Conventional EPR spectra of native and cross-linked F-actin filaments as determined in Fig. 3. The spectrum in (A) was recorded in a cell oriented parallel to H. The spectra in (B) were recorded when the cell is oriented perpendicular to H. The F-actin filaments are (a) unmodified; (b) interstrand cross-links from Cys374 to Lys191; (c) intrastrand cross-links from Gln41 to Cys374. For each sample, the hyperfine spitting constants were measured. The ratio of this quantity determined when the cell is in the parallel orientation to that observed when the cell is in the perpendicular orientation was then calculated, and the resulting values are listed in Table 1.

Table 1. Effect of cross-linking on static order and rotational motion. F-actin samples were centrifuged at 100 000 ***g*** for 2 h at 4 °C to obtain an actin pellet, which was aligned on the surface of a flat cell. The hyperfine splitting constant ($2A'_{zz}$) was measured parallel and perpendicular to the orientation of the actin filaments with respect to the laboratory magnetic field. The 'orientation order' was calculated from the ratio of the hyperfine splitting constants. Smaller order parameter corresponds to larger orientation order. In the table k means the longer axis of the actin filaments.

Sample	$2A'_{zz}$ (mT) H par. k [a]	$2A'_{zz}$ (mT) H per. k	Ratio of hyperfine splitting constants
F-actin	6.835	6.454	0.945
Interstrand cross-linking			
F-actin (Lys191-Cys374)		6.398	0.937
Intrastrand cross-linking			
F-actin (Gln41–Lys113)		6.707	0.983
F-actin (Gln41–Cys374)		6.729	0.986

[a] The hyperfine splitting constant in the parallel orientation was practically the same for all actin samples within the limits of experimental error. The standard deviations are 0.025 mT. H par. k and H per. k mean that the longer axis (k) of the actin filaments was oriented either parallel or perpendicular to the laboratory magnetic field (H).

upon the addition of more HMM. Presumably, the extra HMM shields the probe bound to actin residue Cys374 [6]. Cross-linking within filaments does not fundamentally alter this phenomenon. Because the protein (and its attached probe) are further immobilized by both Gln41–Cys374 and Gln41–Lys113 intrastrand cross-links, the hyperfine splitting constants do increase, an effect observed at all concentrations of added HMM.

To further study the flexibility of the filaments, the mobility of the paramagnetic probe attached rigidly to the filaments was determined at different temperatures (Fig. 5). The Arrhenius principle predicts an inverse dependence of the hyperfine splitting constant upon temperature, a consequence of intramolecular thermal motions. Deviation from a linear dependence could occur when effect other than temperature increase produce changes in the conformation of interacting proteins within the same temperature range. Indeed, the hyperfine splitting constant decreases as the temperature is increased, an effect common to native and cross-linked F-actin. Cross-linking is observed to restrict the mobility of the filaments at all temperatures. In order to explain the linear dependence of $[2A'_{zz}\ (0\ °C) - 2A'_{zz}\ (t\ °C)]$ upon 1000/T, we assume that $2A'_{zz}$ (0 °C) is approximately equal to the rigid limit of the hyperfine splitting constant, $2A^{r}_{zz}$. The rotational correlation time for the bound spin label follows from the Goldman equation [20]. According to the logarithmic formulation thereof, we find that $\ln \tau_2 = b/2A^{r}_{zz} * [2A'_{zz}\ (0\ °C) - 2A'_{zz}\ (t\ °C)] + (\ln a - b)$.

This mathematical relationship is a formal statement of the proportionality between $\ln \tau_2$ and the difference between hyperfine coupling constants. This

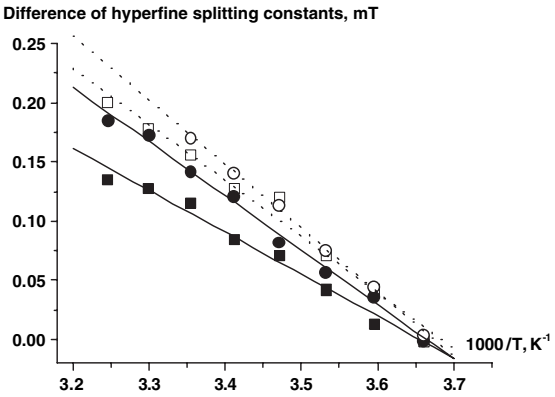

Fig. 5. The difference of the hyperfine splitting constant in miliT graphed against reciprocal temperature (1000/K). EPR spectra were recorded on native actin (○), native actin complexed with myosin fragment S1 (□), cross-linked actin (●), and cross-linked actin complexed with myosin fragment S1 (■). When present, myosin fragment S1 was in a 1 : 5 molar ratio to actin. Solid lines are fitted to values measured on cross-linked F-actin, whereas dotted lines represent those for native filaments.

effect amounts to a decrease of τ_2 as a function of increasing thermal motions within the molecules. According to the Goldman equation $b = -1.36$ and $a = 0.54$ ns, assuming Brownian rotational diffusion. The result shows that the curves follow the Arrhenius relationship It suggests that $\Delta A'_{zz}$ is proportional to changes in the rotational Brownian movement (itself the result of increasing thermal energy). The curves calculated for the native and cross-linked filaments differ by $\Delta 2A'_{zz}$, a measure of the reduction of flexibility. Similar linear relationships among these parameters are observed with the cross-linked and native acto-S1 complexes.

Effects of nucleotides on the interaction of cross-linked samples with myosin fragments

In previous studies, we demonstrated that cross-linking impairs the motor function of actomyosin, therefore in this study we compared the dynamics of actin filaments at different stages of the actomyosin contractile cycle. HMM/adenosine 5′[βγ-imido] triphosphate (AMPPNP) complex was used as HMM/ATP state and HMM/ADP/AlF_4 complex represents a stable analogue of HMM/ADP/P_i state. The half-life of the ADP/AlF_4 complex without actin is 2 days, the presence of actin accelerates decomposition of complex, and the half-life decreases to ~100 min at 25 °C [31] however, this is long enough for this study because after mixing actin and HMM/ADP/AlF_4 complex in the EPR cell, the measurement is completed within 10 min.

The effects of HMM and HMM/nucleotide complexes are studied using conventional and ST EPR techniques. As determined by conventional EPR (Table 2), measured values of $2A'_{zz}$ approach the rigid limit observed with F-actin, however, addition of HMM or HMM/nucleotide complex significantly alters these values. These results agree with earlier observations, and reflect co-operative changes in the F-actin structure [6,7]. Steady-state phosphorescence anisotropy measurements also suggest that the binding of myosin heads to F-actin almost immobilized the rotational motion of the filaments on a microsecond timescale [21,22]. Addition of HMM or HMM/ADP increased the $2A'_{zz}$ values. By contrast, HMM/ADP/AlF_4 slightly decreased that parameter, indicating a different environment for the probe under the weak binding of HMM/ADP/AlF_4 to actin. In the case of cross-linked F-actin, no significant responses were detected by conventional EPR measurement when HMM or HMM/nucleotide complexes were added, because all measured cross-linked actin and actin HMM complexes reached the rigid limit range. The ST EPR spectra of F-actin/HMM and F-actin/HMM/nucleotide complexes, however, showed informative differences (Table 3 and Fig. 6).

Table 2. Interaction of actin with HMM measured by conventional EPR. HMM and HMM saturated with ADP or ADP/AlF_4 were added to F-actin solution (50–100 μM), the molar ratio of HMM to actin was 1–10. After addition of HMM or HMM–nucleotide complexes to F-actin, EPR spectra were taken immediately in the conventional EPR time domain at room temperature. The motional state was characterized by the hyperfine splitting constant ($2A'_{zz}$), measured in mT. The plane of the flat cell was always oriented parallel to the laboratory magnetic field to avoid larger contribution from partially oriented F-actin filaments.

	No addition	HMM	HMM/ADP	HMM/ADP/AlF_4
F-actin	6.807 [a]	6.817	6.816	6.764
Cross-linked F-actin (Gln41–Cys374)	6.852	6.864	6.853	6.863

[a] Values are the means of three determinations in mT, the error of the determinations is 0.02 mT.

Table 3. Comparison of F–actin–HMM interaction by ST EPR. Cross-linked (Gln41–Cys374) and control F-actin solutions were combined with HMM and HMM–nucleotide complexes (the molar ratio of HMM to actin was 1–10). ST EPR spectra were taken in a parallel orientation of the flat cell with respect to the laboratory magnetic field. From the spectra the diagnostic ratio L″/L was estimated. Concentration of the proteins: 80 μM (actin) and 8 μM (HMM).

		Diagnostic ratio L″/L [a]	
		Control	Cross-linked
F-actin alone	Actin	0.860	0.894
Strong-binding state	Actin + HMM	1.114	1.213
	Actin + HMM/ADP	1.085	1.161
Weak-binding state	Actin + HMM/AMP/PNP	1.026	1.080
	Actin + HMM/ADP/AlF_4	1.034	1.285

[a] Spectra were evaluated by at least three runs of the computer program to obtain the estimation of the diagnostic peaks. The SD of L″/L estimated from independent measurements was 0.07 ($n = 5$).

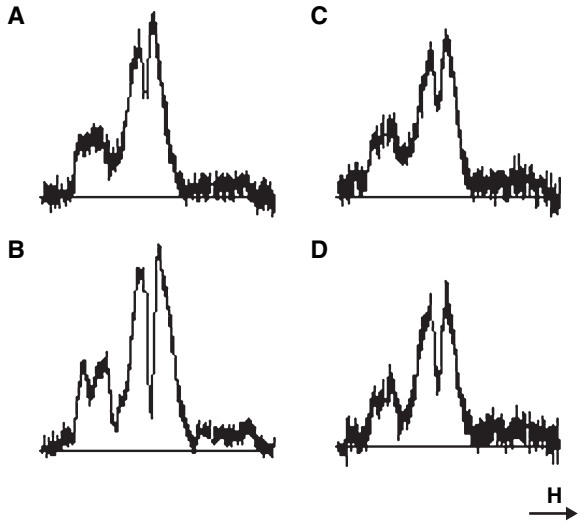

Fig. 6. ST EPR spectra of actin bound by HMM or HMM/ADP/AlF_4 complex. Spectra were recorded on (A) native actin + HMM; (B) native actin + HMM/ADP/AlF_4 complex; (C) cross-linked actin + HMM; (D) cross-linked actin + HMM/ADP/AlF_4 complex. In every case, the molar ratio of HMM to actin was 1 : 10.

The diagnostic ratio of L″/L changed in both the control and cross-linked samples. In the control F-actin samples, there are differences in the motion of the EPR probe when the acto-HMM complex is in a strong and weak binding state, respectively. Under strong binding of HMM and HMM/ADP complex to F-actin the L″/L ratios indicate near equal strong immobilization of the motion. In the weak binding state of F-actin–HMM/AMPPNP and F-actin–HMM/ADP/AlF_4 complexes the motion of the probe is less restricted relative to the strong binding state and there is no difference between the two weak binding complexes. In the case of cross-linked F-actin, the EPR probe behaves similarly under strong binding, whereas the L″/L-values are somewhat higher. We found a remarkable difference, however, under weak binding. The F-actin–HMM/AMPPNP complex behaves similarly to the control sample, but in the F-actin–HMM/ADP/AlF_4 complex there is no decrease in the L″/L-value, it remained as high as it is in the rigor complex. This difference in EPR signal suggests that cross-linking impaired the ability of F-actin filaments to respond to the HMM/ADP/AlF_4-induced dynamic change that we detected in the control actin using both conventional and ST EPR methods. In an earlier study, the interaction of ATP and S1 with actin during activation of myosin S1 ATPase using caged ATP did not produce an increase in rotational motion in the environment of the Cys374 site of actin [8]. In a recent publication the authors argue that in the weak binding state of myosin to actin the heads interact only with one actin protomer [23]. In our experiments HMM was used instead of S1, and the coupling between the two heads was able to induce changes in the flexing motion of the filaments. Spectroscopy and electron microscopy data suggest that myosin head groups attached to actin in the weakly bound state exist in various orientations, and the efficiency of fluorescence energy transfer is much smaller than that observed when myosin and actin combine in a tight-binding state [24–26]. The transition from the intermediate weak-binding state to the strong-binding state requires a conformational change, an intramolecular motion associated with force generation by actomyosin. In molecular simulations that dock one protein upon the other, structural transitions at the acto-S1 interfaces contribute to the overall conformational change that occurs during the power stroke [27]. Cross-links between actin molecules may diminish the necessary conformational flexibility or distort their orientation within the filament. In other studies, we found no significant differences in the rate of ATP hydrolysis, ATP-induced dissociation of actin from the myosin S1 fragment, and ADP dissociation from the acto-S1 complex with cross-linked versus uncross-linked actins [14,15]. Nevertheless, cross-linking actin molecules impair the motor function of actomyosin. This effect may correspond to the above differences in the motion of the EPR probe in the weak-binding state of HMM/ADP/AlF_4 with cross-linked versus native filaments. According to these EPR measurements, cross-linked actin filaments retain their strongly restricted dynamic properties in spite of binding by HMM/ADP/AlF_4, possibly undermining an essential property of the system needed to generate movement. Of course we are interested in the actin–HMM/ADP/AlF_4 complex because it is a model for the ADP/P_i state of the actomyosin system within the ATPase/force-generation cycle. In conclusion, we suggest that the dynamic properties of the actin filaments have an essential role in the motor function of actomyosin, particularly at the prepower stroke stage.

Experimental procedures

Reagents

Synthesis of N-(4-azido-2-nitrophenyl)-putrescine (ANP) and N-(4-azidobenzoyl)-putrescine (ABP) were as described previously [11,12]. Maleimido-TEMPO was from Aldrich Chemical Co. (Milwaukee, WI), and *N*,*N*′-*p*-phenylendima-

leimide (p-PDM), ATP, ADP were from Sigma Chemical Co., (St. Louis, MO). All other reagents were of analytical grade. Ca^{2+}-independent bacterial transglutaminase was a generous gift from K. Seguro (Ajimoto Co. Inc., Kawasaki, Japan).

Proteins

Rabbit skeletal muscle α-actin was isolated from an acetone powder of the hind-leg and back muscles of domestic white rabbits [28]. HMM was prepared by chymotryptic digestion of skeletal muscle myosin as described previously [29].

Chemical modification of actin

In the course the chemical modification of actin, residue Cys374 can react with the spin label as well as the cross-linking agent. Consequently, our procedure yielded actin copolymers in which some monomers were spin-labelled, whereas others were cross-linked (but unlabelled). Subunits with one or the other chemical modification assembled in a random order. Intense EPR signals were detected when 25–30% of actin monomers were spin-labelled, a situation in which ample protein subunits remained unlabelled and available for reaction with the cross-linking agent.

Spin-labelling

F-actin in F buffer (4 mM Tris/HCl, pH 7.6, 0.2 mM ATP, 2 mM $MgCl_2$) was reacted with a 1.5-fold molar excess of maleimido-TEMPO for 2 h at room temperature. Once covalently modified, the F-actin was centrifuged at 100 000 ***g*** for 90 min in a Beckman 55.2 Ti rotor. The resulting pellet was homogenized, and dialysed overnight in G buffer (4 mM Tris/HCl, pH 7.6, 0.2 mM ATP, 0.2 mM $CaCl_2$).

Cross-linking of actin by ABP or ANP

Spin-labelled and unlabelled G-actin were combined in a molar ratio of 1 : 2 at a total concentration of 2 $mg{\cdot}mL^{-1}$. Such 'mixed' G-actin was incubated in the dark with an eightfold molar excess of ABP or ANP in the presence of transglutaminase (0.5 $units{\cdot}mL^{-1}$) for 4 h at room temperature. The portion of the sample labelled on Gln41 was polymerized by addition of $MgCl_2$ (2 mM), enabling it to be pelleted by ultracentrifugation. The actin copolymer – some subunits being covalently modified with the spin label, others with ABP or ANP – was pelleted by centrifugation. It was then homogenized in F buffer and incubated on ice for 1 h under a stream of N_2. Photo-cross linking of double labelled F-actin was carried out as described elsewhere [11,12].

Cross-linking of actin by p-PDM

Maleimido-TEMPO labelled G-actin was mixed with unlabelled G-actin at a molar ratio of 1 : 3, and then polymerized by the addition of $MgCl_2$ (2 mM). Polymerized F-actin, now spin-labelled at some but not all subunits, was cross-linked with the bifunctional reagent p-PDM [30]. For EPR measurements, all samples of the cross-linked F-actin were pelleted and redissolved in F buffer at a final concentration of 0.12–0.14 mM.

Preparation of HMM/ADP/AlF_4^- complex

Trapping of ADP and AlF_4^- by HMM was performed essentially as described in Werber *et al.* [31]. One day before use, 20 μM HMM was incubated for 5 min at 25 °C in 1 mM $MgCl_2$, 20 mM Tris/HCl pH 7.9, 0.2 mM ADP and 5 mM NaF (freshly prepared). After addition of 1 mM $AlCl_3$, the reaction mixture was incubated for an additional 15 min. The sample was then dialysed against 20 mM Tris/HCl pH 7.9, 1 mM $MgCl_2$ at 4 °C or used directly in the EPR analysis as described below.

EPR spectroscopy

Conventional and ST EPR spectra were recorded with an ESP 300E spectrometer (Bruker Biospin, Rheinstetten, Germany). First harmonic in-phase, absorption spectra were obtained using 20 mW microwave power and 100 kHz field modulation with amplitude of 0.15 mT. Second harmonic, 90° out-of-phase absorption spectra were recorded with 63 mW and 50 kHz field modulation of 0.5 mT amplitude detecting the signals at 100 kHz out-of-phase. The 63 mW microwave power corresponds to an average microwave field amplitude of 0.025 mT in the centre region of the standard Zeiss tissue cell (Carl Zeiss, Jena, Germany), and the values were obtained by using the standard protocol of Fajer & Marsh [32]. Actin concentrations in the measuring cell were 80–120 μM, the spectra were recorded at 23 (± 1) °C. Each spectrum was normalized according to the number of unpaired electrons calculated from the corresponding double integral. In order to compare the conventional EPR (CW EPR) spectra of the various actin samples, we measured the difference between their outermost hyperfine extremes ($2A'_{zz}$). This parameter correlates with the rotational motion of the probe in the nanosecond time range. In the very slow time domain ST EPR spectra were recorded and the diagnostic parameter L″/L was used to characterize the motional state.

Acknowledgements

This work was supported by grants T34874, CO123, TS049812 from the Hungarian Scientific Research

Fund (OTKA), and GVOP-3.1.1-2004-0235 grant of National Development Plan.

References

1 Geeves MA & Holmes KC (1999) Structural mechanism of muscle contraction. *Annu Rev Biochem* **68**, 687–728.
2 Zeng W, Conibear PB, Dickens JL, Cowie RA, Wakelin S, Málnási-Csizmadia A & Bagshaw CR (2004) Dynamics of actomyosin interactions in relation to the cross-bridge cycle. *Phil Trans R Soc Lond Biol Sci* **359**, 1843–1855.
3 Yanagida T & Oosawa F (1978) Polarized fluorescence from ε-ATP incorporated into F-actin in myosin-free single fiber: conformation of actin and changes induced in it by heavy meromyosin. *J Mol Biol* **126**, 507–524.
4 Prochniewicz-Nakayama E, Yanagida T & Oosawa F (1983) Studies on conformation of F-actin in muscle fibers in relaxed state, rigor and during contraction using fluorescent phalloidin. *J Cell Biol* **97**, 1663–1667.
5 Borovikov Yu S, Dedova IV, dos Remedios CG, Vikhoreva NN, Vikhorev PG, Avrova SV, Hazlett TL & Van Der Meer BW (2004) Fluorescence depolarization of actin filaments in reconstructed myofibers: The effect of S1 or p-PDM-S1 on movements of distinct areas of actin. *Biophys J* **86**, 3020–3029.
6 Thomas DD, Seidel JC & Gergely J (1979) Rotational dynamics of F-actin in submillisecond time range. *J Mol Biol* **132**, 257–273.
7 Mossakowska M, Belágyi J & Strzelecka-Golaszewska H (1988) An EPR study of the rotational dynamics of actins from striated and smooth muscle and their complexes with heavy meromyosin. *Eur J Biochem* **175**, 557–564.
8 Ostap EM & Thomas DD (1991) Rotational dynamics of spin-labelled F-actin during activation of myosin S1 ATPase using caged ATP. *Biophys J* **59**, 1235–1241.
9 Borejdo J, Shepard A, Dumka D, Akopova I, Talent J, Malka A & Burghardt TP (2004) Changes in orientation of actin during contraction of muscle. *Biophys J* **86**, 2308–2317.
10 Sase I, Miyata H, Ishiwata S & Kinosita K Jr (1997) Axial rotation of sliding actin filaments revealed by single-fluorophore imaging. *Proc Natl Acad Sci USA* **94**, 5646–5650.
11 Hegyi G, Michel H, Shabanowitz J, Hunt DF, Chatterjie N, Healy-Louie G & Elzinga M (1992) Gln-41 is intermolecularly cross-linked to Lys-113 in F-actin by N-(4-azidobenzoyl) -putrescine. *Protein Sci* **1**, 132–144.
12 Hegyi G, Mák M, Kim E, Elzinga M, Muhlrad A & Reisler E (1998) Intrastrand cross-linked actin between Gln-41 and Cys-374. I. Mapping of sites cross-linked in F-actin by N-(4-azido-2-nitophenyl) -putrescine. *Biochemistry* **37**, 17784–17792.
13 Elzinga M & Phelan JJ (1984) F-actin is intermolecularly cross-linked by *N*,*N*'-*p*-phenylen-dimaleimide through lysine-191 and cysteine-374. *Proc Natl Acad Sci USA* **81**, 6599–6602.
14 Kim E, Bobkova E, Miller CJ, Orlova A, Hegyi G, Egelman EH, Muhlrad A & Reisler E (1998) Intrastrand cross-linked actin between Gln-41 amd Cys-374. III. Inhibition of motion and force generation with myosin. *Biochemistry* **37**, 17801–17809.
15 Kim E, Bobkova E, Hegyi G, Muhlrad A & Reisler E (2002) Actin cross-linking and inhibition of actomyosin motor. *Biochemistry* **41**, 86–93.
16 Cooke R & Morales MF (1971) Interaction of globular actin with myosin subfragments. *J Mol Biol* **60**, 249–261.
17 Pope D, Lednev VV & Jahn W (1987) Methods of preparing well-oriented sols of F-actin containing filaments suitable for X-ray diffraction. *J Mol Biol* **197**, 679–684.
18 Burley RW, Seidel JC & Gergely J (1971) The stochiometry of the reaction of the spin labeling of F-actin and the effect of orientation of spin-labelled F-actin filaments. *Arch Biochem Biophys* **146**, 597–602.
19 Naber N, Lorentz M & Cook R (1994) Orientation of spin-probes attached to Cys 374 on actin in oriented gels. *J Mol Biol* **236**, 703–709.
20 Goldman SA, Bruno GV & Freed JH (1972) Estimating slow motional rotational correlation times for nitroxides by electron spin resonance. *J Phys Chem* **76**, 1858–1860.
21 Ng Choi-man & Ludescher RD (1994) Microsecond rotational dynamics of F-actin in actoS1 filaments during ATP hydrolysis. *Biochemistry* **33**, 9098–9104.
22 Prochniewicz E & Thomas DD (1997) Perturbations of functional interaction with myosin induced long-range allosteric and cooperative structural changes in actin. *Biochemistry* **36**, 12845–12853.
23 Prochniewicz E, Walseth TF & Thomas DD (2004) Structural dynamics of actin during active interaction with myosin. Different effects of weakly and strongly bound myosin heads. *Biochemistry* **43**, 10642–10652.
24 Gu J, Xu S & Yu LC (2002) A model of cross-bridge attachment to actin in the AM.ATP state based on X-ray diffraction from permeabilized rabbit psoas muscle. *Biophys J* **82**, 2123–2133.
25 Iwamoto H, Oiwa K, Suzuki T & Fujisawa T (2001) X-Ray diffraction evidence for the lack of stereospecific protein interactions in highly activated actomyosin complex. *J Mol Biol* **305**, 863–874.
26 Xu J & Root DD (2000) Conformational selection during weak binding at the actin and myosin interface. *Biophys J* **79**, 1498–1510.
27 Root DD, Stewart S & Xu J (2002) Dynamic docking of myosin and actin observed with resonance energy transfer. *Biochemistry* **41**, 1786–1794.
28 Spudich JA & Watt S (1971) Regulation of rabbit skeletal muscle contraction I. Biochemical studies of interac-

tion of the tropomyosin–troponin complex with actin and proteolytic fragments of myosin. *J Biol Chem* **246**, 4866–4871.
29 Margossian SS & Lowey S (1982) Preparation of myosin and its subfragments from rabbit skeletal muscle. *Methods Enzymol* **85**, 55–71.
30 Knight P & Offer G (1978) *p-NN′*-Phenylenbismaleimide, a specific cross-linking agent for F-actin. *Biochem J* **175**, 1023–1032.
31 Werber MM, Peyser YM & Muhlrad A (1992) Characterization of stable berilium fluoride, aluminium fluoride and vanadate containing myosin subfragment 1-nucleotide complexes. *Biochemistry* **31**, 7190–7197.
32 Fajer P & Marsh D (1982) Microwave and modulation field inhomogenities and effect of cavity Q in saturation transfer EPR spectra. Dependence of sample size. *J Magn Res* **49**, 212–224.